Syst. Biol. 49(3):592–612, 2000

Phylogenetic Relationships Among the Phrynosomatid Sand Lizards Inferred from Mitochondrial DNA Sequences Generated by Heterogeneous Evolutionary Processes

JAMES WILGENBUSCH[1] AND KEVIN DE QUEIROZ[2]

[1]*Laboratory of Molecular Systematics, MRC 534, MSC, Smithsonian Institution, Washington, D.C. 20560, USA; E-mail: jim@lms.si.edu*

[2]*Department of Vertebrate Zoology, National Museum of Natural History, Smithsonian Institution, Washington, D.C. 20560, USA; E-mail: dequeirk@nmnh.si.edu*

Abstract.—Nucleotide sequences of the mitochondrial protein coding cytochrome *b* (cyt *b*; 650 bp) and small-subunit 12S ribosomal RNA (~350 bp) genes were used in analyses of phylogenetic relationships among extant phrynosomatid sand lizards, including an examination of competing hypotheses regarding the evolution of "earlessness." Sequences were obtained from all currently recognized species of sand lizards as well as representatives of the first and second outgroups and analyzed using both parsimony and likelihood methods. The cyt *b* data offer strong support for relationships that correspond with relatively recent divergences and moderate to low support for relationships reflecting more ancient divergences within the clade. These data support monophyly of the "earless" taxa, the placement of *Uma* as the sister taxon to the other sand lizards, and monophyly of all four taxa traditionally ranked as genera. All well-supported relationships in the 12S phylogeny are completely congruent with well-supported relationships in the cyt *b* phylogeny; however, the 12S data alone provide very little support for deeper divergences. Phylogenetic relationships within species are concordant with geography and suggest patterns of phylogeographic differentiation, including the conclusion that at least one currently recognized species (*Holbrookia maculata*) actually consists of more than one species. By independently optimizing likelihood model parameters for various subsets of the data, we found that nucleotide substitution processes vary widely between genes and among the structural and functional regions or classes of sites within each gene. Therefore, we compared competing phylogenetic hypotheses, using parameter estimates specific to those subsets, analyzing the subsets separately and in various combinations. The hypothesis supported by the cyt *b* data was favored over rival hypotheses in all but one of the five comparisons made with the entire data set, including the set of partitions that best explained the data, although we were unable to confidently reject ($P < 0.05$) alternative hypotheses. Our results highlight the importance of optimizing models and parameter estimates for different genes or parts thereof—a strategy that takes advantages of the strengths of both combining and partitioning data. [Combining data; cytochrome *b*; maximum likelihood; mitochondrial DNA; phrynosomatidae; phylogeny; 12S RNA; sand lizards.]

The phrynosomatid sand lizards form a clade of 8–10 currently recognized species distributed in arid and semiarid regions of western North America (de Queiroz, 1989). This group has interested systematic biologists because of a continuing controversy about the phylogenetic relationships among four taxa traditionally recognized as genera: *Callisaurus* (zebra-tailed lizards, one currently recognized species), *Cophosaurus* (greater earless lizards, one species), *Holbrookia* (lesser earless lizards, three species), and *Uma* (fringe-toed lizards, three to five species). Among the four alternative hypotheses proposed for the relationships among these taxa (Fig. 1), the main differences concern first, whether the first taxon to diverge was *Uma* (Fig. 1, topologies I and III) or *Holbrookia* (Fig. 1, topology IV), and second, whether *Cophosaurus* is the sister group of *Holbrookia* (Fig. 1, topologies I and II), with which it shares the derived character of a concealed tympanic membrane, or of *Callisaurus* (Fig. 1, topology III and IV), to which it bears a greater overall resemblance. The second disagreement forms the basis of a related controversy about whether the concealed tympanic membrane ("earless" condition) of *Cophosaurus* and *Holbrookia* has been inherited from a common ancestor or is the result of convergent or parallel evolution.

Most recent studies (e.g., Etheridge and de Queiroz, 1988; de Queiroz, 1989, 1992; Porter et al., 1994; Changchien, 1996; Reeder and Wiens, 1996) have supported the early divergence of *Uma* and the sister group relationship of *Cophosaurus* and *Holbrookia* (Fig. 1, topology I). Moreover, a review of all the data that had been presented up to 1989 (de Queiroz, 1989) revealed first, that most of the similarties between *Cophosaurus* and *Callisaurus* are retained ancestral features, and

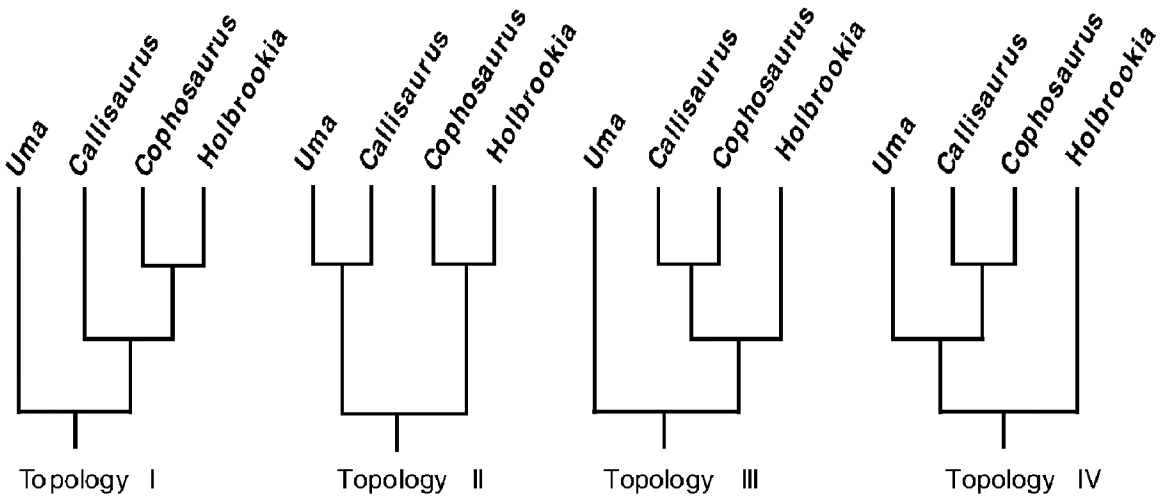

FIGURE 1. Alternative hypotheses of higher-level relationships among the sand lizards. Topology I (Savage, 1958; Cox and Tanner, 1977; Etheridge and de Queiroz, 1988; de Queiroz, 1989, 1992; Reeder and Wiens, 1996; Changchien, 1996); topology II (Mittleman, 1942; Smith, 1946); topology III (Norris, 1958; Earle, 1961, 1962); topology IV (Axtell, 1958; Clarke, 1965; Adest, 1978).

second, that there were no known derived characters shared by those two taxa that are not also shared by either *Uma*, *Holbrookia*, or both of these taxa. Nevertheless, we wished to evaluate hypotheses about sand lizard phylogeny with new data in the form of DNA sequences and new analytical capabilities that have recently become available.

Like many recent molecular phylogenetic studies, ours is based on data from structurally and functionally separate genes (i.e., cytochrome *b* [cyt *b*] and 12S RNA). Currently there is disagreement about how multiple data sets, including those based on different genes, should be analyzed—that is, separately or combined (reviewed by de Queiroz et al., 1995; Hillis et al., 1996). For the most part, opposition to combining data sets occurs when those data sets are thought to have been generated by distinctly different processes. Bull et al. (1993), for example, generated simulated nucleotide sequence data on the same tree under two distinct models and showed that parsimony analysis of the combined data sets resulted in a poor estimate of the true tree. In the context of parsimony, weighting for position (e.g., codon position, stems vs. loops) and transformation (e.g., transitions vs. transversions) has been used to accommodate different underlying processes (Chippindale and Wiens, 1994); however, that approach lacks an explicit basis for assessing which weighting scheme provides the best explanation of the data (Huelsenbeck et al., 1994).

In contrast, likelihood has an explicit basis for assessing the ability of different models to explain the data (see Swofford et al., 1996), because likelihood scores (the probability of the data, given the hypothesis) are comparable across models. Moreover, statistical tests can be used to assess the significance of the differences in likelihood scores between models, which is desirable because overly deterministic models, though they inevitably improve the likelihood score also increase sampling variance and may ultimately decrease accuracy (Cunningham et al., 1998). For these reasons, we used an approach based on likelihood to select a model from a set of progressively more-restrictive models (i.e., those with progressively greater numbers of estimated parameters), using that model as the basis for subsequent phylogenetic analyses. We also took advantage of the additive properties of likelihood scores (Edwards, 1972) and the existence of previously specified alternative phylogenetic hypotheses to assess the amount of support among four rival hypothesis, using the entire data set but allowing for heterogeneity in the models applied to its various subsets.

MATERIALS AND METHODS

Taxon Sampling

Samples of fresh liver or muscle tissue were collected from 26 phrynosomatid sand lizards, representing all 10 currently

TABLE 1. The taxonomic designation, code, museum number, and collecting locality of the specimens used in the study. Subspecies taxonomy of *Holbrookia maculata* follows Axtell (1958). Nonstandard abbreviations: KdQ = Kevin de Queiroz; RRM = Richard R. Montanucci (field catalogues).

Taxon			Code	Museum no.	Collecting locality
Sand lizards					
Callisaurus	*draconoides*	*bogerti*	CDBO	ROM 14970	México; Sinaloa; vic. Mazatlan
		carmenensis	CDCA	ROM 14182	México; Baja California; vic. San Ignacio
		crinitis	CDCR	MVZ 214832	México; Baja California; vic. Guerrero Negro
		myurus	CDMY	MVZ 214751	USA; Nevada; Mineral Co.
		rhodostictus	CDRH	MVZ 214739	USA; California; Inyo Co.
		ssp.	CDSS	ROM 15034	México; Sonora; vic. Bahõa Kino
		ventralis	CDVE	LSUMZ 48811	USA; New Mexico, Hidalgo Co.
Cophosaurus	*texanus*	*scitulus*	CTSC	MVZ 214711	USA; Arizona; Pima Co.
		texanus	CTTE	USNM 315499	USA; Texas; Blanco Co.
Holbrookia	*lacerata*	*lacerata*	HLLA	USNM 315500	USA; Texas; Concho Co.
		subcaudalis	HLSU	USNM 315503	USA; Texas; McMullen Co.
	propinqua	*propinqua*	HPRO	MVZ 214863	USA; Texas; Nueces Co.
	maculata	*bunkeri*	HMBU	USNM 337740	USA; New Mexico; Luna Co.
		canipi	HMCA	MVZ 214801	USA; New Mexico; McKinley Co.
		elegans	HMEL	ROM 14964	México; Sinaloa; vic. Mazatlan
		flavilenta	HMFL	MVZ 21814	USA; Arizona; Cochise Co.
		maculata	HMMA	MVZ 214806	USA; New Mexico; Chaves Co.
		rutlweni	HMRU	USNM 337752	USA; New Mexico; Otero Co.
		thermophila	HMTH	CAS 174377	USA; Arizona; Cochise Co.
Uma	*exsul*		UEXS	ROM 15315	México; Durango, vic. Hwy 47
	inornata		UINO		USA; California; Riverside Co.
	notata	*notata*	UNNO	MVZ 214799	USA; California; Imperial Co.
	notata	*rufopunctata*	UNRU	ROM 13919	México; Sonora; vic. Puerto Peñasco
	paraphygas		UPAR	ROM 15089	México; Durango, vic. Mapimõ
	scoparia		USC1	ROM 14637	USA; California, San Bernardino Co.
	scoparia		USC2	MVZ 214784	USA; California; San Bernardino Co.
First outgroup					
Phrynosoma	*hernandesi*		PHER	RRM 2470	USA; Colorado; Weld Co.
	platyrhinos		PPLA	KdQ 057	USA; California; no further data
Second outgroup					
Sceloporus	*jarrovii*		SJAR	KdQ 036	USA; Arizona; Cochise Co.
Urosaurus	*ornatus*		UORN	MVZ 214658	USA; Arizona; Yavapai Co.
Uta	*stansburiana*		USTA	CAS 178153	USA; Arizona; Pima Co.

vic., in the vicinity of.

recognized species (Table 1). An effort was made to sample geographic variation, particularly within polytypic species. In addition, five specimens representing five distantly related species within the first and second outgroups—based on the phylogenies of Etheridge and de Queiroz (1988) and Reeder and Weins (1996)—were included in the analysis. These taxa were used to root the trees in the various phylogenetic analyses. Tissues were frozen in liquid nitrogen in the field and maintained at −80°C in the laboratory until DNA was extracted.

DNA Isolation, Amplification, and Sequencing

Genomic DNA was extracted from ~10 mg of frozen liver tissue by incubating the samples in STE buffer (0.4 M NaCl, 10 mM Tris-HCl pH 7.5, 10 mM EDTA), 20% sodium dodecyl sulfate and proteinase K (10 μg/μl) for at least 12 hours at 55°C. DNA was purified by extraction with phenol/chloroform, precipitated with ethanol, and resuspended in 15–100 μl of TMS–EDTA buffer (Hillis et al., 1990).

The polymerase chain reaction (PCR) (~50 ng DNA; 0.4 mM primer each; 0.15 mM dNTP; 5 μl of 10× buffer; 1.5 mM $MgCl_2$; 1.25 to 2.5 units of Taq polymerase, and distilled H_2O up to 50 μl) (96°C, 45 sec; 45–50°C, 45 sec; 72°C, 60 sec) was used to amplify fragments of two mitochondrial genes, a 650-bp fragment of the cyt *b* gene and a fragment of ~350 bp of the ribosomal 12S gene. Two equal sized (~400 bp) portions of the cyt *b* fragment were independently amplified

using two pairs of primers: L14841: 5′-AAA AAGCTTCCATCCAACATCTCAGCATGA TGAAA-3′, H15149: 5′-AAACTGCAGCCC CTCAGAATGATATTTGTCCTCA3′ and L15066: 5′-AATAAGCTTTTAAAGAAACAT GAAA(T/C)ATTGGAGTA-3′, H15498: 5′-A AACTGCAGGGAATAAAGTTATCTGGGT CTC-3′; numbers in the primer names refer to positions in the human sequence (Anderson et al., 1981). A single pair of 12S primers was used: 5′-AAACTGGGATTA GATACCCCACTAT-3′ and 5′-GAGGGTGA CGGGCGGTGTGT-3′ (Reeder, 1995). The double-stranded PCR products were purified with 20% polyethylene glycol, dye-labeled using a dye terminator cycle sequencing reaction kit (ABI PRISM; Amplitaq DNA polymerase), and sequenced on an automated sequencer (models 373a and 373 stretch; Applied Biosystems, Inc.). The absence of indels in the cyt *b* sequences made it possible to align these sequences unambiguously by eye. A preliminary alignment of the 12S consensus sequences was made using CLUSTAL W (Thompson et al., 1994) under the default settings. Improvements to the initial alignment were made by eye, using published models of secondary structure for a variety of taxa (Sullivan et al., 1995; Hickson et al., 1996; Richards and Moore, 1996). Sequences are deposited with GenBank under the accession numbers AF194215–AF194276.

Phylogenetic Analysis

We used maximum likelihood to select models of sequence evolution, to refine parameter estimates used in phylogeny reconstruction, and to select optimal trees (see Swofford et al., 1996). Processes governing DNA sequence evolution and their effects on the estimation of phylogenies have been well documented (e.g., Collins et al., 1995; Sullivan et al., 1995; Sullivan, 1996; Wakely, 1996; Yang, 1996a). Consequently, explicit models of sequence evolution have been developed in an attempt to compensate for potentially confounding effects for use under a likelihood approach to phylogeny reconstruction. Likelihood models have been tested under a diverse set of simulated conditions (Gaut and Lewis, 1995) and have been shown to outperform other methods when data are simulated under more complex (and arguably more realistic) conditions (Huelsenbeck, 1995; Yang, 1996b). Furthermore, the ability to objectively evaluate evolutionary models under likelihood is of great importance in light of the general recognition that the processes governing molecular evolution are not uniform across taxa (Wolfe et al., 1989; Martin and Palumbi, 1993; Simon et al., 1996; Nielsen, 1997) and that using oversimplified or arbitrary models to infer phylogeny has undesirable consequences (Felsenstein, 1978; Yang, 1996b; Sullivan and Swofford, 1997; Cunningham et al., 1998; Naylor and Brown, 1998).

Phylogenetic analyses of the nucleotide sequence data were conducted using test versions 4.0d64–65 of PAUP*, written by David L. Swofford. We generated initial topologies for the cyt *b* and 12S sequences, using heuristic searches (10 random stepwise additions of taxa and tree bisection–reconnection [TBR] branch swapping) under parsimony with equal weighting for both codon positions and classes of nucleotide substitutions. We then evaluated the likelihood of several nested models of sequence evolution (see below) on the parsimony topologies to determine which model and associated parameter values yielded the highest probability for the sequence data. The model and associated parameters that maximized the likelihood were next used in a heuristic search (as-is stepwise addition of taxa and TBR branch swapping) under the likelihood criterion. This process was reiterated with subsequent likelihood topologies until the same topology or set of topologies was found in successive searches.

We explored four substitution models: Jukes–Cantor (JC; Jukes and Cantor, 1969), Kimura two-parameter (K2P; Kimura, 1980), Hasegawa–Kishino–Yano (HKY; Hasegawa et al., 1985), and the general time reversible (GTR; the REV of Yang, 1994a) (see Swofford et al. [1996] for model descriptions). Each substitution model was first evaluated by assuming no rate heterogeneity among sites and then with three combinations of rate heterogeneity parameters: (1) the I of Hasegawa et al. (1985), in which a proportion of sites were considered invariable (variable sites were assumed to follow an equal rates model); (2) the gamma (Γ) of Yang (1994b), in which all sites were assumed to follow a discrete gamma-distributed rates model; and (3) I + Γ (Gu et al., 1995; Waddel and Penny, 1996), in which some sites were considered invariable and the variable sites were

assumed to follow a gamma-distributed rates model. Rate heterogeneity parameters were optimized under each substitution model; therefore, 16 models were evaluated (i.e., 4 substitution models × 4 combinations of rate parameters) for each data set and topology. A likelihood ratio test (Cox and Hinkley, 1974) was used to determine whether models differed significantly in their likelihood scores. Because each model is a special case of the most general GTR + I + Γ model, this amounted to determining whether increasing the number of parameters estimated from the data (i.e., relaxing the model restrictions) significantly improved the ability of the model to explain the data. The test statistic is assumed to be χ^2 distributed, with the degrees of freedom equal to the difference in the number of parameters between the two models. Theoretically, the use of the χ^2 distribution is valid only when the likelihoods of the nested models are computed on the true topology (Yang et al., 1995a); however, Yang et al. (1995b) have suggested that uncertainty about phylogeny is not a practical problem because differences between substitution models are most often greater than differences between topologies. Because it was impossible for us to know whether we were assessing the true topology, we compared the 16 nested models using several alternative topologies representing rival phylogenetic hypotheses (Fig. 1) to determine whether the preferred model was consistent across the alternative topologies.

We assessed the support for the putative clades identified by parsimony and likelihood searches using nonparametric bootstrap resampling (Felsenstein, 1985). Under the parsimony criterion, 200 bootstrap replicates were performed on the cyt *b* and 12S data sets using heuristic searches (simple stepwise addition of taxa and TBR branch swapping), both with equal weights for character positions and with step matrices to down-weight transitions 10:5, 10:4, 10:3, and 10:2 (i.e., 2:1, 2.5:1, ~3.3:1, 5:1). The transversion/transition (tv:ti) weighting schemes were selected because they formed a narrow range around the transition bias estimated under maximum likelihood (i.e., ~2.8). Under the likelihood criterion, 100 bootstrap replicates were performed on the cyt *b* and 12S data sets using heuristic searches (as-is stepwise addition of taxa and TBR branch swapping) under the GTR + I + Γ model. For both cyt *b* and 12S bootstrap searches, the GTR + I + Γ model parameters were fixed to the parameter values estimated on the tree found in the final iteration of the successive approximations procedure described above.

We also used our data to evaluate the relative merits of four previously proposed phylogenetic hypotheses (Fig. 1)—one of which corresponds to our best estimate of sand lizard phylogeny based on the cyt *b* sequences. The successive approximation approach described above was used to find optimal topologies, with the branching order among the four taxa traditionally recognized as genera constrained to correspond to each of the previously proposed phylogenies. The cyt *b* data were used to find the optimal topologies under the various constraints because these data provided greater resolution for relationships reflecting deeper sand lizard divergences. We then optimized models and parameter estimates for both gene fragments together, for each gene fragment separately, and for structurally and functionally defined regions or classes of sites within each gene fragment (i.e., stems and loops for 12S, codon positions for cyt *b*).

In this approach, support for each topology can be evaluated for each data partition. In addition, because the measure of support (i.e., likelihood) is additive (see Edwards, 1972), overall support for each hypothesis can be assessed as the sum of the estimates for the individual data partitions (Adachi and Hasegawa, 1992; Huelsenbeck and Bull, 1996). However, by estimating parameter values separately for each data partition, we run the risk of overparameterizing the model. It therefore becomes important to know whether the additional model parameters help to provide a better general fit to the data, or just fit random variation. To this end, a likelihood ratio test was used to determine whether partitioning the data significantly improved the overall likelihood score. Here again the likelihood ratio is χ^2 distributed, the degrees of freedom being equal to the difference in the number of parameters used to estimate the two likelihood scores. Because model parameters were optimized for each data partition, the total number of model parameters was equal to the number of branch lengths ($2T - 3$, where T is the number of terminal taxa) plus the number of substitution parameters, all multiplied by the number of data partitions. Finally, we

evaluated the significance of the observed differences between the likelihood scores of alternative phylogenetic hypotheses, using the method proposed by Kishino and Hasegawa (1989). All site likelihood scores were generated using test version 4.0d64 of PAUP*, and the standard errors of the differences between topologies were generated using SAS (SAS Institute, 1990).

In addition, the amino acid translation of cyt *b* nucleotide sequences was used to evaluate the four competing hypothesis (Fig. 1) under a likelihood framework. We used the program PROTML in the MOLPHY package (Adachi and Hasegawa, 1992) to evaluate the likelihood of the four topologies under the transition probability matrix of Jones et al. (1992), using as an estimate of the amino acid frequencies those observed in the cyt *b* fragment (JTT-F option in PROTML). Of the alternative likelihood models available in PROTML, we chose the JTT-F model because it provided the best fit to the amino acid–coded data. PROTML was used to calculate the standard error of the difference between competing hypotheses and thus to compare those hypotheses using the test of Kishino and Hasegawa (1989).

RESULTS

Sequence Variation

Cytochrome b.—In all, 650 nucleotide positions were aligned, of which 274 were variable and 240 were parsimony-informative. No insertions or deletions (indels) were observed. 202 (93%) of the third codon positions were variable compared with 60 (28%) of first the codon and 12 (6%) of the second codon positions. All of the third position substitutions were synonymous, whereas 60% of the first codon and 100% of the second codon substitutions resulted in amino acid substitutions. In all, 38 (17%) of the amino acid positions were variable. Observed differences in nucleotide base composition among taxa were not significant, as indicated by the χ^2 homogeneity test (first position $\chi^2 = 5.71$, $P = 1.0$; second position $\chi^2 = 0.35$, $P = 1.0$; third position, $\chi^2 = 29.34$, $P = 1.0$; and all sites, $\chi^2 = 3.84$, $P = 1.0$). On the other hand, the frequencies of the four bases varied overall and for each codon position (Table 2), as indicated by the base compositional bias (Bias C) of Irwin et al. (1991). First codon positions showed the lowest bias (C = 0.042), whereas high T and low A and G frequencies at second positions resulted in an intermediate bias (C = 0.236), and high A and low G frequencies at third positions resulted in the most bias (C = 0.293) among codon positions. General patterns of bias for each codon position observed here are similar to those reported for mitochondrial genes sequences from birds (Kornegay et al., 1993; Nunn and Cracraft, 1996; Nunn et al., 1996), mammals (Irwin et al., 1991), and collembolans (Frati et al., 1997). Corrected (likelihood under the GTR + I + Γ model) pairwise distances (Table 3) between and within currently recognized sand lizard species ranged between 0.009 and 0.508 and between 0.002 and 0.208, respectively.

12S rRNA.—Nucleotide sequence length varied between 336 and 352 bp for the 31 taxa examined. After inserting 29 gaps to accommodate the alignment of conservative regions, 367 positions were aligned. A total of 19 positions could not be confidently aligned because of multiple indels, and these positions were not considered in subsequent analyses. Indels were only inferred in single-stranded regions (loops) of the 12S molecule. Not including indels, 105 characters were variable, of which 76 were parsimony-informative. More loop positions (37%) than stem (25%) positions were variable. Alignment of complementary stem positions for each sequence resulted in 50% A–U, 38% C–G, 9% G–U, 1% A–C, and 2% miscellaneous base pair combinations. The relatively high number of noncanonical G–U pairs in the stems of vertebrate ribosomal RNA genes is not uncommon (Kraus et al., 1992; Dixon and Hillis, 1993; Kjer, 1995), perhaps because they are thought to have the least effect on the destabilization of secondary structure (James et al., 1988) and may even be selectively advantageous (Rousset et al., 1991). Base composition did not vary significantly among taxa (loop $\chi^2 = 9.26$, $P = 1.0$ χ^2; stem $\chi^2 = 4.02$, $P = 1.0$; and all sites $\chi^2 = 2.74$, $P = 1.0$). However, the pattern of base compositional bias differed between stem and loop regions (Table 2). In particular, the loop region was A-rich and G/T-poor (C = 0.301), whereas the stem region showed very little base compositional bias (C = 0.041). This pattern of base compositional bias for the 12S gene fragment is similar to the pattern observed among Galapagos iguanas (Rassmann, 1997) and a diverse sample of

TABLE 2. The GTR + I + Γ model parameters for each data set maximized on the MP topology giving the highest likelihood score (see Fig. 1). The transitions headers (C↔T and A↔G) are in bold and the G↔T transformation rate is fixed at 1. Base frequencies are the mean of those observed for each data set.

	Substitution rates					Rate parameters		Observed base frequencies			
	C↔T	**A↔G**	A↔C	A↔T	C↔G	I	G	A	C	G	T
Cytochrome *b*											
All	41.045	14.653	5.521	3.293	0.520	0.537	1.582	0.29	0.25	0.14	0.32
Codon 1	98.855	25.524	7.690	14.065	3.00E-07	0.677	2.450	0.26	0.22	0.25	0.27
Codon 2	3.16×10^{9}	1.60×10^{9}	3.85×10^{8}	9.32×10^{-3}	5.46×10^{-5}	0.790	0.488	0.19	0.23	0.15	0.43
Codon 3	4.259	6.363	0.195	0.231	1.336	0	2.727	0.43	0.29	0.03	0.25
12S											
All	40.904	11.506	3.536	4.098	0.316	0.496	0.717	0.36	0.22	0.19	0.23
Loop	33.495	5.089	1.859	3.590	0.604	0.404	0.764	0.46	0.22	0.13	0.19
Stem	28.556	24.553	4.330	0.905	0	0.178	0.194	0.26	0.22	0.25	0.27
Cyt *b* and 12S	53.426	15.561	5.963	4.395	0.568	0.540	1.110	0.32	0.24	0.16	0.28

TABLE 3. Maximum likelihood pairwise genetic distances (GTR + I + Γ) for the outgroup taxon *Phrynosoma hernandesi* (PHER) and all sand lizard ingroup taxa. The cyt *b* distances are below the diagonal and the 12S distances are above it. Intraspecific comparisons (based on the current taxonomy) are outlined.

	TAXA																											
	PHER	UPAR	UEXS	USC1	USC2	UNRU	UNNO	UINO	CDSS	CDBO	CDCR	CDCA	CDVE	CDMY	CDRH	CTTE	CTSC	HLLA	HLSU	HPRO	HMEL	HMTH	HMMA	HMCA	HMFL	HMRU	HMBU
PHER	—	0.188	0.214	0.133	0.133	0.147	0.127	0.147	0.195	0.195	0.215	0.208	0.214	0.214	0.214	0.195	0.182	0.191	0.218	0.236	0.249	0.241	0.171	0.224	0.188	0.215	0.207
UPAR	0.436	—	0.019	0.099	0.099	0.089	0.075	0.089	0.105	0.105	0.112	0.114	0.119	0.119	0.119	0.138	0.112	0.112	0.101	0.107	0.126	0.118	0.097	0.127	0.094	0.116	0.109
UEXS	0.449	0.189	—	0.109	0.109	0.104	0.091	0.104	0.132	0.132	0.147	0.153	0.144	0.155	0.155	0.159	0.135	0.140	0.118	0.143	0.152	0.144	0.127	0.168	0.133	0.156	0.149
USC1	0.439	0.278	0.253	—	0.000	0.016	0.013	0.016	0.102	0.102	0.135	0.123	0.118	0.127	0.127	0.119	0.111	0.122	0.123	0.162	0.140	0.142	0.117	0.160	0.130	0.153	0.146
USC2	0.443	0.275	0.250	0.002	—	0.016	0.013	0.016	0.102	0.102	0.135	0.123	0.118	0.127	0.127	0.119	0.111	0.123	0.123	0.163	0.141	0.142	0.117	0.161	0.130	0.154	0.147
UNRU	0.451	0.295	0.256	0.113	0.115	—	0.000	0.000	0.098	0.098	0.121	0.114	0.093	0.102	0.102	0.114	0.111	0.122	0.123	0.147	0.145	0.137	0.112	0.155	0.125	0.148	0.141
UNNO	0.447	0.281	0.261	0.124	0.127	0.020	—	0.000	0.075	0.075	0.102	0.095	0.075	0.084	0.084	0.103	0.111	0.097	0.097	0.116	0.113	0.104	0.105	0.123	0.094	0.117	0.110
UINO	0.444	0.283	0.263	0.113	0.115	0.013	0.009	—	0.098	0.098	0.121	0.114	0.093	0.102	0.102	0.114	0.111	0.122	0.123	0.147	0.145	0.137	0.112	0.155	0.125	0.148	0.141
CDSS	0.367	0.421	0.351	0.337	0.340	0.357	0.348	0.351	—	0.000	0.037	0.022	0.033	0.033	0.033	0.140	0.121	0.124	0.098	0.117	0.120	0.106	0.088	0.095	0.081	0.102	0.096
CDBO	0.392	0.369	0.316	0.332	0.336	0.331	0.321	0.324	0.038	—	0.037	0.022	0.033	0.033	0.032	0.140	0.121	0.124	0.098	0.117	0.120	0.106	0.088	0.095	0.081	0.102	0.096
CDCR	0.426	0.392	0.365	0.365	0.361	0.369	0.358	0.361	0.093	0.104	—	0.009	0.016	0.009	0.009	0.140	0.126	0.124	0.113	0.132	0.144	0.130	0.108	0.120	0.101	0.122	0.116
CDCA	0.399	0.399	0.358	0.345	0.342	0.345	0.328	0.338	0.097	0.113	0.038	—	0.012	0.006	0.006	0.141	0.130	0.128	0.111	0.142	0.144	0.130	0.105	0.113	0.098	0.120	0.113
CDVE	0.408	0.393	0.356	0.357	0.361	0.356	0.339	0.342	0.107	0.111	0.117	0.112	—	0.006	0.006	0.152	0.138	0.137	0.110	0.146	0.151	0.137	0.123	0.131	0.116	0.138	0.131
CDMY	0.385	0.391	0.368	0.330	0.334	0.372	0.363	0.359	0.101	0.110	0.094	0.096	0.057	—	0.000	0.148	0.133	0.137	0.120	0.146	0.151	0.137	0.114	0.122	0.107	0.129	0.122
CDRH	0.393	0.383	0.358	0.327	0.330	0.367	0.357	0.353	0.096	0.104	0.097	0.098	0.058	0.011	—	0.148	0.133	0.137	0.120	0.146	0.151	0.137	0.114	0.122	0.107	0.129	0.122
CTTE	0.466	0.429	0.403	0.359	0.362	0.361	0.371	0.368	0.348	0.338	0.291	0.302	0.306	0.319	0.324	—	0.041	0.146	0.132	0.148	0.117	0.116	0.130	0.177	0.149	0.175	0.167
CTSC	0.468	0.413	0.389	0.357	0.361	0.378	0.409	0.392	0.340	0.342	0.288	0.299	0.310	0.336	0.335	0.055	—	0.118	0.105	0.101	0.084	0.093	0.105	0.129	0.103	0.127	0.120
HLLA	0.516	0.474	0.464	0.435	0.438	0.402	0.426	0.415	0.336	0.338	0.339	0.350	0.326	0.332	0.325	0.363	0.350	—	0.033	0.115	0.096	0.106	0.079	0.097	0.076	0.096	0.090
HLSU	0.423	0.497	0.446	0.395	0.399	0.406	0.453	0.427	0.269	0.307	0.302	0.315	0.294	0.291	0.302	0.326	0.296	0.127	—	0.103	0.090	0.095	0.082	0.108	0.087	0.106	0.101
HPRO	0.515	0.474	0.443	0.387	0.391	0.366	0.370	0.358	0.369	0.367	0.316	0.337	0.354	0.369	0.362	0.353	0.342	0.307	0.297	—	0.057	0.058	0.049	0.069	0.044	0.060	0.056
HMEL	0.492	0.394	0.338	0.356	0.353	0.330	0.333	0.329	0.340	0.328	0.312	0.342	0.341	0.340	0.335	0.283	0.306	0.282	0.275	0.161	—	0.019	0.037	0.052	0.051	0.051	0.047
HMTH	0.474	0.420	0.328	0.342	0.345	0.310	0.328	0.324	0.317	0.298	0.296	0.330	0.303	0.316	0.318	0.240	0.281	0.288	0.271	0.200	0.125	—	0.037	0.052	0.044	0.044	0.040
HMMA	0.446	0.446	0.376	0.379	0.375	0.370	0.382	0.379	0.297	0.305	0.290	0.316	0.327	0.301	0.293	0.288	0.255	0.272	0.262	0.189	0.207	0.176	—	0.012	0.012	0.012	0.009
HMCA	0.456	0.490	0.360	0.361	0.358	0.342	0.367	0.364	0.315	0.324	0.302	0.316	0.333	0.310	0.303	0.324	0.304	0.275	0.252	0.168	0.195	0.196	0.052	—	0.025	0.019	0.015
HMFL	0.494	0.508	0.404	0.374	0.377	0.355	0.380	0.376	0.321	0.329	0.300	0.321	0.340	0.307	0.310	0.315	0.298	0.286	0.258	0.175	0.199	0.190	0.059	0.044	—	0.012	0.009
HMRU	0.470	0.484	0.360	0.354	0.357	0.329	0.353	0.349	0.315	0.323	0.304	0.324	0.335	0.304	0.309	0.318	0.294	0.281	0.248	0.170	0.206	0.200	0.060	0.045	0.025	—	0.003
HMBU	0.494	0.506	0.395	0.385	0.382	0.359	0.377	0.381	0.340	0.342	0.309	0.330	0.348	0.330	0.335	0.324	0.288	0.296	0.251	0.187	0.208	0.208	0.063	0.050	0.034	0.014	—

phrynosomatid lizards (Reeder, 1995). Corrected (likelihood: GTR + I + Γ) pairwise distances (Table 3) between and within currently recognized sand lizard species ranged between 0 and 0.177 and between 0 and 0.052, respectively.

Nucleotide Substitution Patterns

Cytochrome b.—Nucleotide substitutions are generally considered in terms of changes within the two structural classes of nucleotides (purines and pyrimidines), that is, in terms of transitions and transversions. However, pairwise estimates of nucleotide substitution patterns among phrynosomatid lizards suggest that G↔A transitions may occur less frequently than in other vertebrates (Reeder, 1995). The plot of observed differences versus corrected distances (from Table 3) suggests that G↔A transitions do not match the pattern exhibited by C↔T transitions; instead, they more closely approximate the curves for the A↔C and A↔T transversions (Fig. 2a). Pairwise estimates of nucleotide substitutions are problematic in that they do not take multiple substitutions into consideration and therefore tend to underestimate transitions at rapidly evolving sites (see Wakely, 1996). However, topology-based estimates using a model of substitution that accommodates among-site rate heterogeneity show that G↔A transition rates are roughly half of C↔T transition rates (Table 2), indicating that the recognition of only two classes of substitutions (i.e., transitions and transversions) oversimplifies the substitution process. Furthermore, likelihood models with six substitution rate categories (GTR) as opposed to two (K2P or HKY) had markedly higher likelihood scores for all of the topologies examined ($p < 0.0001$) (Fig. 3a).

12S rRNA.—Both pairwise and topology-based estimates of nucleotide substitution

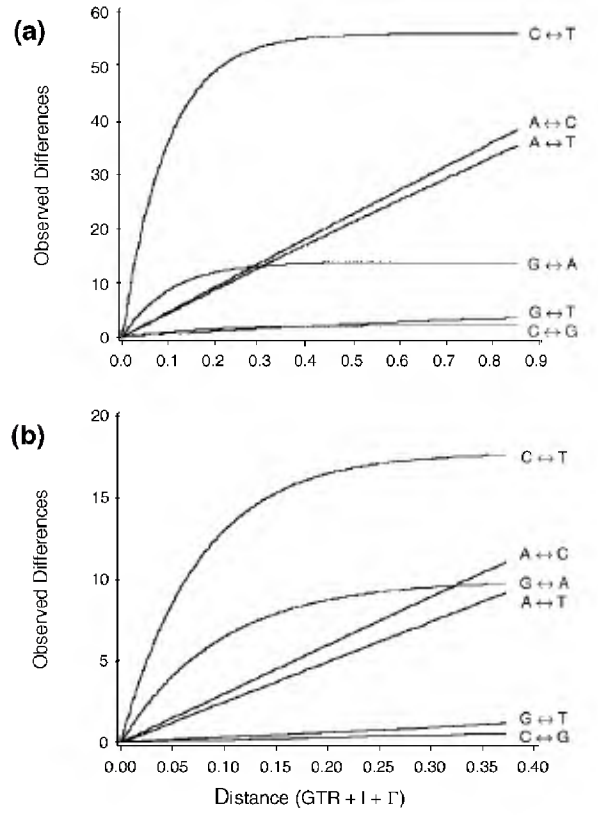

FIGURE 2. Observed pairwise differences plotted as a function of the maximum likelihood pairwise distances under the GTR + I + Γ model. Lines were fitted by using a negative exponential function (SAS, 1990). (a) Cytochrome *b*. (b) 12S RNA.

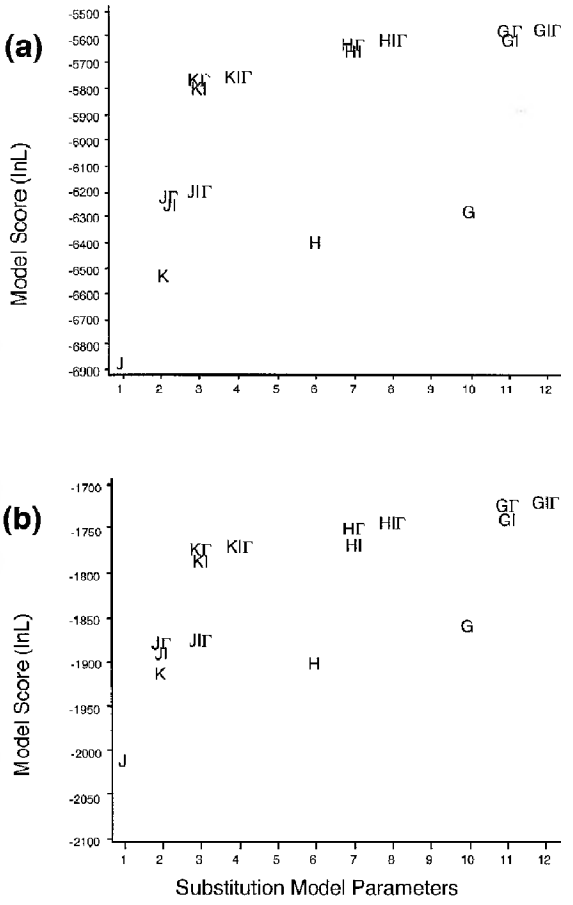

FIGURE 3. The likelihood scores for the 16 models of sequence evolution on the final ML tree for data plotted as a function of the number of substitution model parameters. Substitution models are represented by single characters: J = Jukes–Cantor; K = Kimura two-parameter; H = Hasegawa–Kishino–Yano; and G = general time reversible. Characters following the substitution models represent among-site rate heterogeneity parameters: I = proportion of invariable sites, Γ = gamma. (a) Cytochrome *b*. (b) 12S.

rates suggest that, as in the case of cyt *b*, classification of substitutions into two classes (transitions and transversions) oversimplifies the substitution process. Observed pairwise nucleotide differences plotted against corrected distances (from Table 3) show that A↔G transitions occur at frequencies more similar to certain classes of transversions (Fig. 2b) (Reeder, 1995). Similarly, topology-based estimates indicate that G↔A transition rates are substantially lower than those for C↔T transitions, particularly in the loop regions (Table 2), and likelihood models with six substitution rate categories (GTR) as opposed to two (K2P or HKY) have markedly higher likelihood scores for all of the topologies examined ($p < 0.0001$) (Fig. 3b).

Optimal Trees

Cytochrome b.—Parsimony analysis of the cyt *b* data with equal weights for both codon positions and base transformations resulted in three most-parsimonious (MP) topologies (length = 1,160, Consistency Index [CI] = 0.3464 excluding uninformative characters) (Fig. 4a). Parsimony searches using step matrices to downweight transitions favored one of the three equal-weight MP topologies. Nevertheless, all three MP topologies were used to evaluate the 16 models of sequence evolution described above under the likelihood criterion. The GTR + I + Γ model had the highest likelihood score for each of the three MP topologies. Moreover, despite increased variance from the estimation of additional parameters, the difference between the GTR + I + Γ likelihood score (−lnL = 5544.36) and that of the next best model (GTR + Γ, −lnL = 5582.22) was significant ($\chi^2 = 75.92$, df = 1, $P < 0.0001$) for the most likely parsimony topology. A heuristic search using the GTR + I + Γ model parameters optimized on the single most likely parsimony topology resulted in the same single tree (Fig. 5). Again, the GTR + I + Γ model had the highest likelihood score (−lnL = 5543.606), which was significantly higher ($\chi^2 = 76.80$, df = 1, $P < 0.0001$) than the score of the next best model (GTR + Γ, −lnL = 5582.01) (Fig. 3a). Additional heuristic searches with parameters optimized on successive maximum likelihood (ML) trees did not change the branching order from that of the original ML topology.

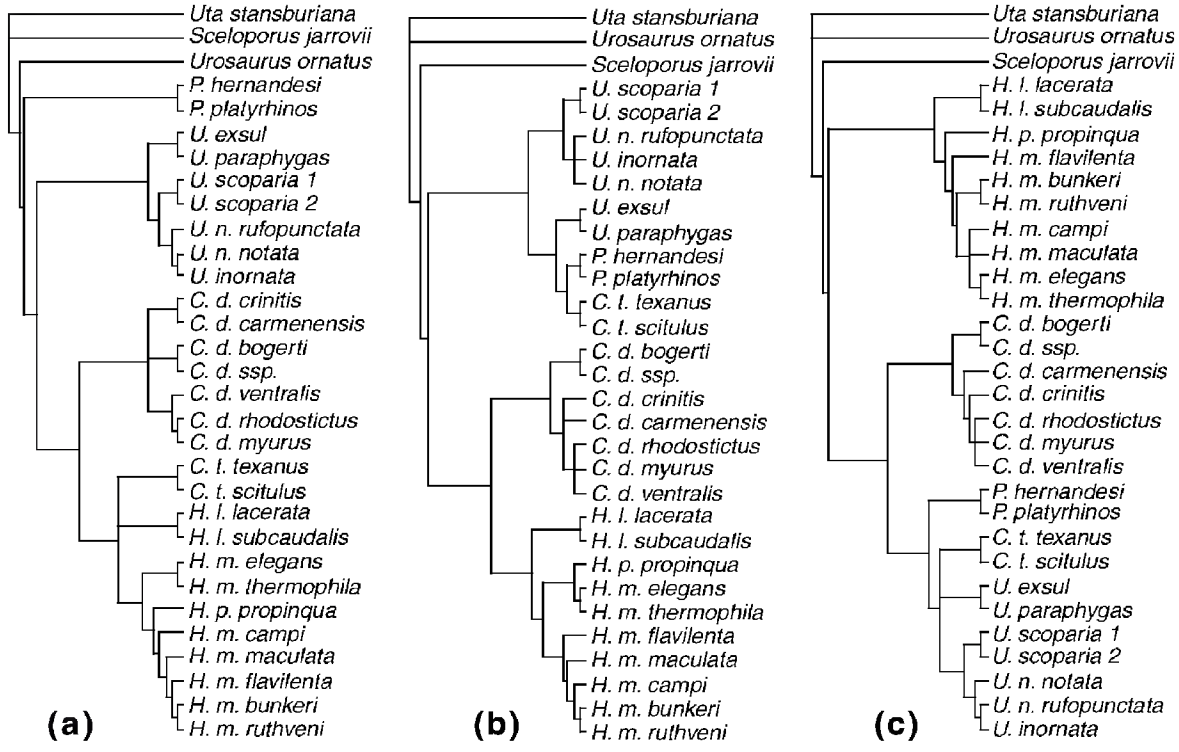

FIGURE 4. The strict consensus trees for: (a) three MP trees for the cyt *b* data, (b) six MP trees for the 12S data, and (c) 15 ML trees for the 12S data.

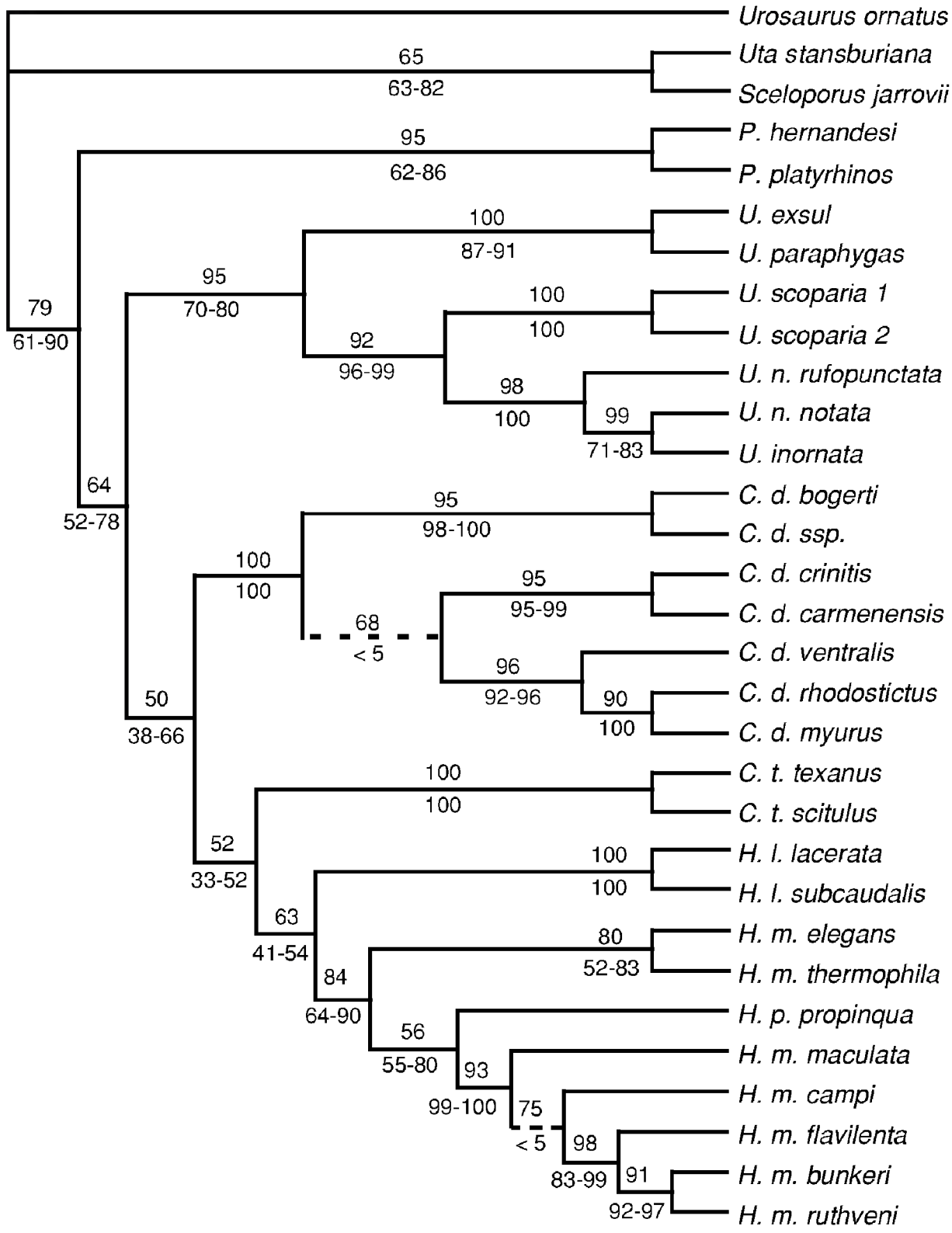

FIGURE 5. Phylogenetic relationships among sand lizards based on likelihood and parsimony analyses of the cytochrome *b* data. The numbers above each node represent the proportion of 100 likelihood bootstrap replicates found under the GTR + I + Γ model of sequence evolution. Numbers below each node represent the range of parsimony bootstrap proportions for 200 replicates when using equal weights and transitions downweighted by 10:5, 10:4, 10:3, and 10:2. The tree is the majority rule bootstrap consensus tree for the likelihood analysis. The majority rule bootstrap consensus trees for the various parsimony analyses are identical except for the branches indicated by dashed lines.

The estimation of model parameters used in phylogeny reconstruction is influenced to some extent by the initial topology on which the parameters are optimized (Yang, 1994b; Sullivan et al., 1996). Therefore, we optimized model parameters on MP topologies constrained to conform to three alternative phylogenetic hypotheses (Fig. 1, topologies II–IV). In all cases, subsequent unconstrained searches using the model parameters optimized on the constrained topologies converged on the same tree that had been found by the search using the model parameters optimized on the most likely parsimony topology.

Bootstrap resampling of the cyt *b* data according to parsimony (equal weights and various ti:tv weighting schemes) and likelihood (GTR + I + Γ) criteria produced nearly concordant topologies (Fig. 5). In general, increasing the weight of transversions increased the bootstrap values for nodes representing deeper divergences, although there is no objective criterion for assessing which ti:tv weighting scheme best explains the data under parsimony. In addition, model selection under likelihood indicates that the data are explained best by a more complicated model—one involving six substitution classes as well as invariant sites and rate variation among variable sites. Therefore, although we present the range of bootstrap values under parsimony, hereafter we emphasize the results obtained under likelihood.

12S rRNA.—Parsimony analysis of the 12S data with equal weights for both character positions and base transformations resulted in six equally MP trees (length = 262, CI = 0.4784 excluding uninformative characters) (Fig. 4b). All six MP trees were used to evaluate the 16 models of sequence evolution under the likelihood criterion. The GTR + I + Γ model had the highest likelihood score for each of the six MP topologies. The score for the GTR + I + Γ model (−lnL = 1717.64) was significantly better ($\chi^2 = 8.48$, $P = 0.0036$) than that of the next best model (−lnL = 1721.88; GTR + Γ) for the most likely parsimony topology. A heuristic search using the GTR + I + Γ model parameters optimized on the most likely parsimony topology resulted in 15 ML topologies (Fig. 4c). Exploring models of evolution given the 15 ML trees again yielded a score for the GTR + I + Γ model (−lnL = 1711.70) that was significantly better ($\chi^2 = 6.22$, $P = 0.0126$) than that of the next best model (−lnL = 1714.81; GTR + Γ) (Fig. 3b). Another heuristic search with the refined GTR + I + Γ parameters yielded the same 15 ML topologies as the previous search.

The parsimony (equal weights and various differential tv:ti weighting schemes) and likelihood (GTR + I + Γ) bootstrap analyses for the 12S data give roughly concordant amounts of support for the resolved nodes (bootstrap proportions >50%) in a generally poorly resolved phylogeny (Fig. 6). Both parsimony and likelihood analyses of the 12S rRNA data show very little support for the deepest nodes in the tree. Rather, those data are more informative regarding the shallower nodes.

Alternative Phylogenetic Hypothesis

We limited our evaluation of alternative hypotheses using partition-specific models to four previously proposed topologies (Fig. 1), one of which (Fig. 1, topology I) corresponds to the MP and ML trees found in unconstrained analyses of our cyt *b* data (Fig. 5). The basal ingroup relationships found in the unconstrained parsimony and likelihood analysis of the 12S data (Fig. 4b and 4c) were not included in this evaluation because the bootstrap analyses (Fig. 6) indicated that the 12S data provided little support for those relationships. We also evaluated both the 12S and cyt *b* topologies with the alternative data set, using the Kishino–Hasegawa (K-H) test (Kishino and Hasegawa, 1989), and found that the cyt *b* data rejected ($P < 0.0001$) the 12S topology but the 12S data could not reject ($P = 0.0975$) the cyt *b* topology. Both gene fragments are physically linked on the mitochondrial genome and therefore must share a common history. It follows that at least one of the gene fragments is giving an incorrect estimation of the phylogeny, and both bootstrap analyses and the K-H test suggest that the misleading fragment is 12S. Although the structural and functional constraints imposed on the 12S molecule could be responsible for the incongruent phylogenies (Simon et al., 1996; Sullivan, 1995, 1996), the relatively small size of the 12S gene fragment we sequenced may also explain its apparent incongruence with the cyt *b* data as well as the poor support that it provides for the basal ingroup relationships.

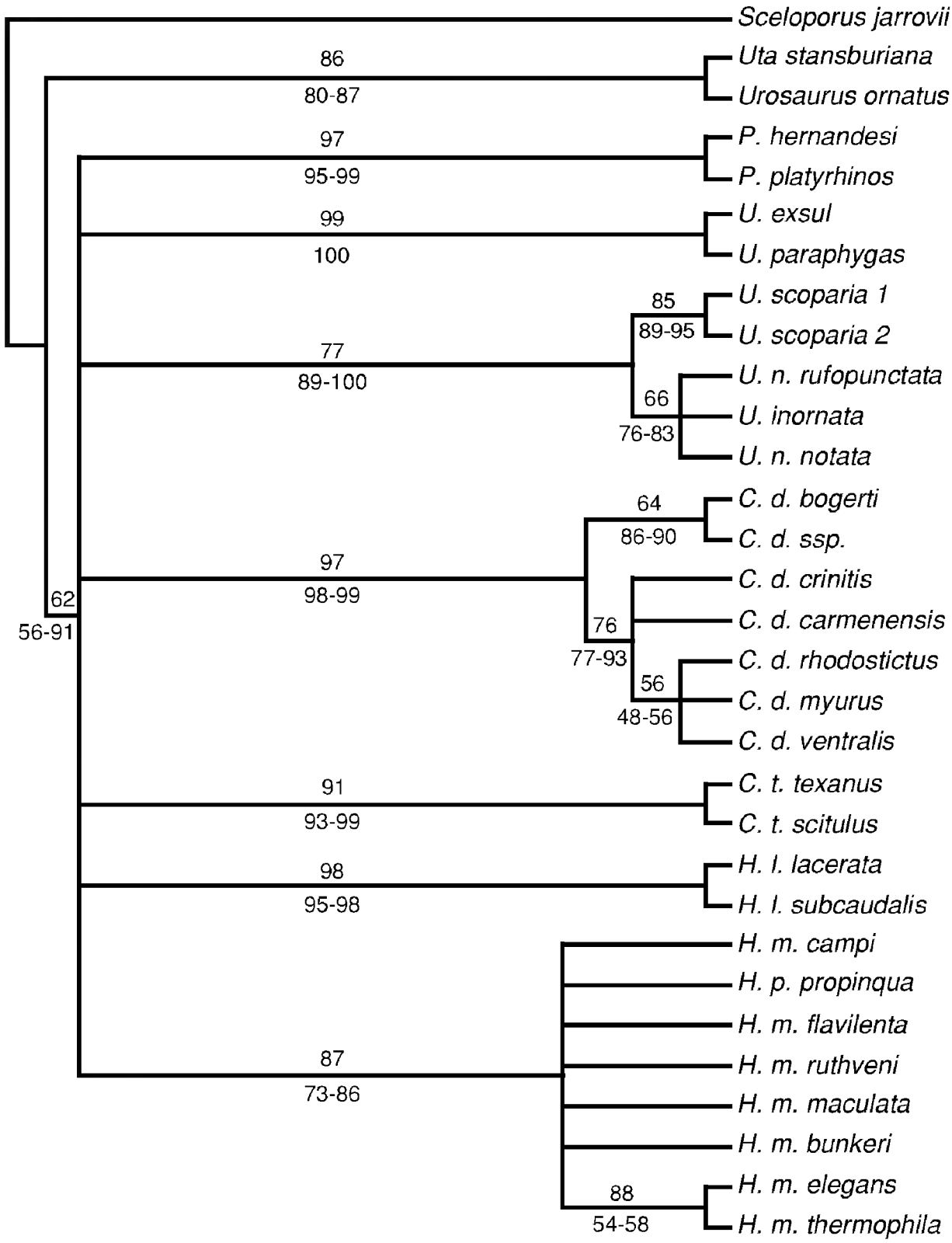

FIGURE 6. Phylogenetic relationships among the sand lizards based on likelihood and parsimony analyses of the 12S data. The numbers above each node represent the proportion of 100 likelihood bootstrap replicates found under the GTR + I + Γ model of sequence evolution. Numbers below each node represent the range of parsimony bootstraps proportions for 200 replicates using equal weights and transitions downweighted by 10:5, 10:4, 10:3, and 10:2. The tree is the majority rule bootstrap consensus tree for the likelihood analysis. The majority rule bootstrap consensus trees for the various parsimony analyses are identical except for the resolution of three additional clades within *Holbrookia*.

TABLE 4. Negative log likelihood scores of topologies I–IV (Fig. 1) under the GTR + I + Γ model for each of the data partitions and combinations thereof. Differences between the log likelihood scores of topology I and topologies II–IV are given in parentheses, followed by the SEs of the differences. The highest likelihood value for each data partition is given in bold. The results of likelihood ratio test, used to determine whether estimating model parameters on the individual data partitions significantly increases the model fit as measured by the log likelihood score, are given for the various combinations of the entire data set. Each combination of partitions for the entire data set is compared to the same data set with one less partition.

		Hypothesis			
Data set	*N*	Top I	Top II	Top III	Top IV
Cytochrome *b*					
Unpartitioned	650	**5543.61**	5546.99 (−3.38), 3.44	5546.97 (−3.36), 3.20	5552.02 (−8.41), 5.42
Codon pos. 1 (C1)	217	**1185.82**	1186.15 (−0.33), 1.01	1186.59 (−0.77), 1.74	1187.07 (−1.25), 1.86
Codon pos. 2 (C2)	217	389.68	391.97 (−2.29), 2.32	386.47 (3.21), 2.63	**386.18** (3.50), 3.34
Codon pos. 3 (C3)	217	**3534.29**	3537.64 (−3.35), 3.25	3536.34 (−2.05), 2.46	3541.16 (−6.87), 4.76
C1 + C2 + C3	650	5109.79	5115.76 (−5.07), 4.12	**5109.4** (0.39), 4.00	5114.41 (−4.62), 6.10
Amino acids	216	**1266.9**	1272.0 (−5.1), 6.1	1268.7 (−1.8), 4.5	1269.0 (−2.1), 4.7
12S					
Unpartitioned	348	1733.78	1733.27 (0.51), 0.87	1733.95 (−0.17), 0.87	**1732.11** (1.67), 2.85
Loop	180	**977.13**	**977.13** (0.00), 0.01	980.22 (−3.09), 3.09	978.97 (−1.84), 3.09
Stem	168	**697.26**	**697.26** (0.00), 0.00	**697.26** (0.00), 0.00	**697.26** (0.00), 0.00
Loop + stem	348	**1674.39**	**1674.39** (0.00), 0.00	1677.48 −(3.09), 2.98	1676.23 (−1.84), 3.91
All data					
Unpartitioned	998	**7358.06**	7360.88 (−2.82), 3.13	7361.16 (−3.10), 3.03	7364.38 (−6.32), 5.62
Cyt *b* + 12S	998	**7277.39**	7280.26 (−2.87), 3.55	7280.92 (−3.53), 3.31	7284.13 (−6.74), 6.12
$\chi^2_{67} = 161.34$	$P < 0.00001$				
Cyt *b* + stem + loop	998	**7218.00**	7221.38 (−3.38), 3.44	7224.45 (−6.45), 4.36	7228.25 (−10.25), 6.68
$\chi^2_{67} = 118.78$	$P = 0.0001$				
C1 + C2 + C3 + 12S	998	6844.47	6849.04 (−4.57), 4.21	**6843.35** (1.12), 4.09	6846.51 (−2.04), 6.74
$\chi^2_{67} = 747.06$	$P < 0.00001$				
C1 + C2 + C3 + loop + stem	998	**6784.18**	6790.15 (−5.97), 4.12	6786.88 (−2.70), 4.98	6790.64 (−6.46), 7.25
$\chi^2_{67} = 120.58$	$P = 0.00008$				

We evaluated each of the four alternative topologies (Fig. 1), using each separate data partition, combinations of partitions, and the amino acid sequence of the cyt *b* molecule (Table 4). Topology I (*Uma* (*Callisaurus* (*Cophosaurus*, *Holbrookia*))) alone received the highest likelihood score for the unpartitioned cyt *b* fragment, the first and third codon positions, the amino acid sequences, and four of the five combinations of partitions using all of the data. Topology I also received the tied highest likelihood score for the loop positions and the combination of loop and stem positions. Topology III was favored by the combination of the individual cyt *b* codon positions and by the combination of the individual codon positions plus the unpartitioned 12S fragment. Second codon positions and the unpartitioned 12S fragment favored topology IV. Topology II was not uniquely favored by any of the data partitions, though it had the tied (with topology I) highest likelihood score for loop positions and loop plus stem positions. The stem positions alone were unable to discriminate among the alternative topologies.

Based on results of the likelihood ratio test, separately optimizing branch lengths and model parameters for different data partitions significantly improved the cumulative likelihood score for all combinations of data partitions relative to the unpartitioned data (Table 4), and the data set with the most partitions explained the data best. Because these comparisons were limited to topologies chosen a priori, the question remains whether better topologies exist. Technological limitations prevented us from searching for optimal trees using combined but partitioned data. Although searching for trees using the combined but unpartitioned cyt *b* plus 12S data sets under the GTR + I + Γ model yielded a novel optimal topology (Fig. 7a), the likelihood of this topology given the unpartitioned data is only 1.74 units greater than that of topology I. In contrast, when model parameters are optimized separately for each of the partitions, the cumulative likelihood score of the optimal tree for the unpartitioned data (i.e., −lnL 6789.93) (Fig. 7a) is 5.75 units less than that of the optimal topology (i.e., topology I).

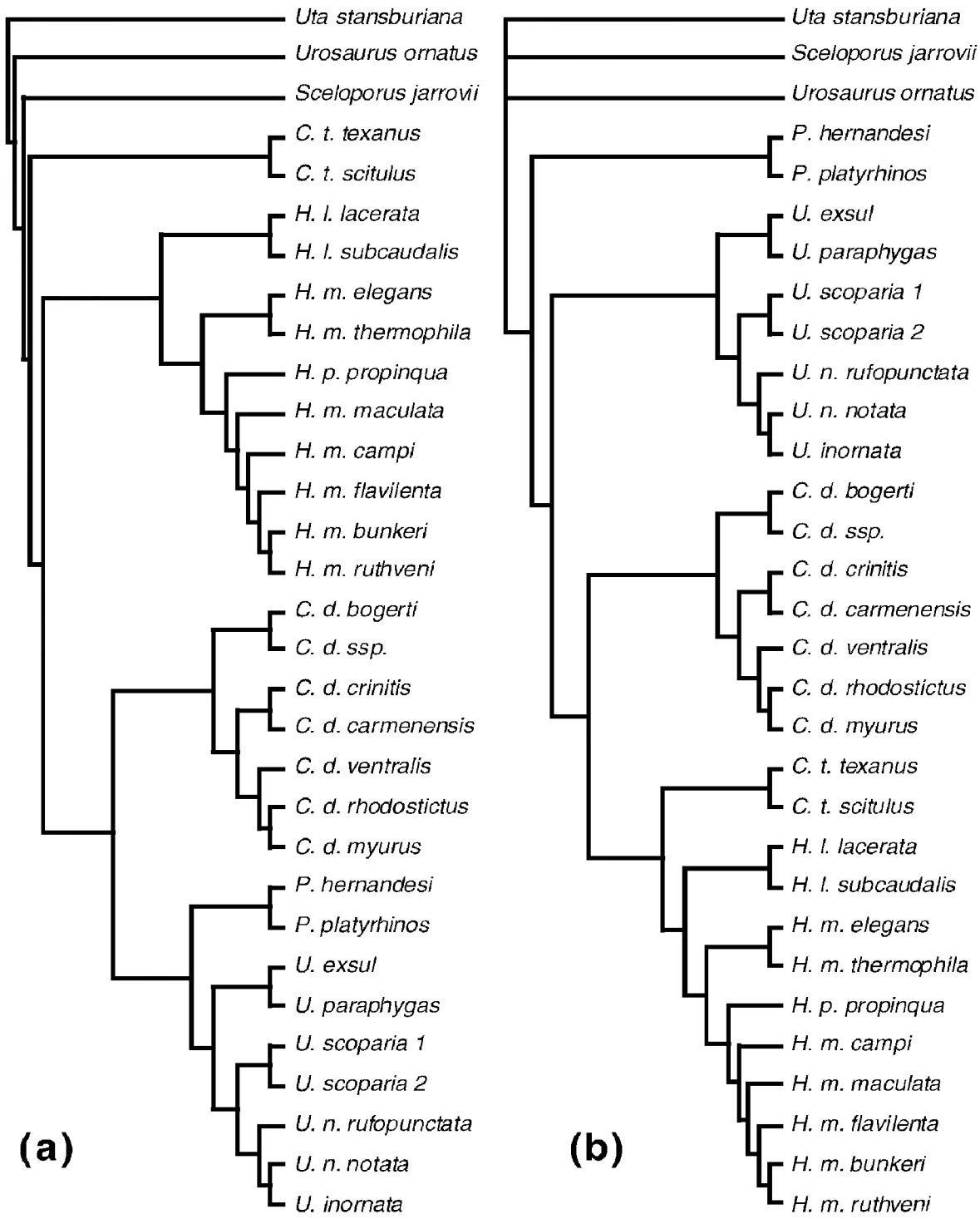

FIGURE 7. Phylogenetic relationships among the sand lizards based on the likelihood and parsimony analyses of the combined but unpartitioned cyt *b* and 12S data. (a) The single ML topology under the GTR + I + Γ model of sequence evolution (−lnL = 7356.34). (b) The strict consensus of the two MP topologies under equal weights for both codon positions and classes of nucleotide substitutions (length = 1434).

Because the data consist of partial gene sequences, it is instructive to estimate the number of nucleotides necessary to confidently (i.e., $P < 0.05$) reject the alternative hypotheses. In particular, we are interested in knowing whether the number of nucleotides needed to reject the alternative hypotheses is greater than the total number in the gene. We can roughly estimate the sample size needed because the mean of the site-likelihood differences is proportional to the sample size and the standard error is proportional to the

square root of the sample size (Kishino and Hasegawa, 1989). For 12S RNA, Simon et al. (1996) demonstrated large differences in substitutional pattern and evolutionary rates between the 3′ and 5′ ends of the molecule. Because our estimate of the number of sites necessary to confidently reject competing hypotheses assumes roughly the same amount of variability as observed in the sequences already collected, we confined our estimate to the cyt *b* gene. We estimated that 2,586 bp are necessary to confidently reject topology II relative to topology I; 2,496 bp to reject topology III; and 1,037 bp to reject topology IV. Based on these estimates, the entire cyt *b* gene (~1,130 bp, Kumazawa et al., 1998) might be sufficient to reject topology IV, but it will probably be necessary to collect data from an additional gene to reject the other two competing hypotheses.

DISCUSSION

Higher-Level Relationships

Four alternative hypotheses have been proposed to describe higher level ("intergeneric") phylogenetic relationships among extant sand lizard taxa, referred to here as topologies I–IV (Fig. 1). Our analyses of two mitochondrial DNA gene fragments favor the phylogenetic relationships among sand lizard "genera" first proposed by Savage (1958)—topology I (Fig. 1)—and later supported by Cox and Tanner (1977), Etheridge and de Queiroz (1988), de Queiroz (1989, 1992), Changchien (1996), Reeder and Wiens (1996), and in part Porter et al. (1994). In this hypothesis, *Uma* is the sister group of all other sand lizards, and the "earless" lizards, *Holbrookia* and *Cophosaurus*, are sister taxa. These relationships are favored by four of the five analyses, on the basis of all of our sequence data, including the best estimate (i.e., C1 + C2 + C3 + stem + loop), although the alternative hypotheses (topologies II–IV) cannot be rejected with a high level of confidence (i.e., $P < 0.05$). The hypothesis that places *Holbrookia* as the sister taxon to all other sand lizards (topology IV) is least favored by the mtDNA sequences examined in this study. The tree constrained to conform to this hypothesis has the lowest likelihood score in all but one of the comparisons that used all of the data. The constrained part of the topology also has no nodes in common with the favored topology (topology I). In addition, this is the only hypothesis that might be rejected with the entire nucleotide sequence of the cyt *b* gene. It is more difficult to discriminate between the favored hypothesis and the other two alternative hypotheses (topologies II and III), both of which have nodes in common with the favored hypothesis.

Although topology IV is favored by the second codon positions of the cyt *b* molecule, the likelihood estimate is based on only 12 variable sites, all of which require an amino acid substitution. Of these sites, only one favors topologies III and IV over topologies I and II—and thus a sister group relationship between *Cophosaurus* and *Callisaurus* rather than between *Cophosaurus* and *Holbrookia*—on the basis of the individual site likelihood scores. All of the *Cophosaurus* and *Callisaurus* specimens and a single *Holbrookia* specimen (HMCA) have thymine at this position; the other samples all have cytosine. Moreover, nonsynonymous substitutions at the first position of this codon result in a pattern of shared amino acids that does not correspond perfectly to the pattern of shared nucleotides at the second position of the codon. *Cophosaurus* and the single *Holbrookia* specimen (HMCA) share valine, *Callisaurus* is characterized by isoleucine, a single *Uma* specimen (UPAR) is characterized by threonine, and all the other samples share alanine. Nevertheless, under the JTT transition model (Jones et al., 1992; see Methods), the single-site likelihood scores for this codon still rank topologies III and IV ahead of topologies I and II, in agreement with the site likelihood scores for the second position of this codon. The point is that this particular nucleotide site is singularly responsible for the rank order of the alternative topologies for the second position data, a ranking that is contradicted by both the nucleotide and amino sequence data for the full cyt *b* fragment, which rank topology I highest. When this single character was removed and the four topologies were again evaluated with the second position data, the rank order of the topologies changed and the likelihood of the difference between the three highest-ranking hypotheses decreased (topology I, −374.59; topology II, −378.91; topology III, −373.99; and topology IV, −375.19).

The debate about whether *Cophosaurus* shares a more recent common ancestor

with *Callisaurus* or with *Holbrookia* and thus whether the "earless" condition in *Cophosaurus* and *Holbrookia* is synapomorphic versus homoplastic has a long history (Mittleman, 1942; Smith, 1946; Axtell, 1958; Norris, 1958; Savage, 1958; Earle, 1961, 1962; Clarke, 1965; Cox and Tanner, 1977; Adest, 1978; Blackburn, 1978; Etheridge and de Queiroz, 1988; de Queiroz, 1989, 1992). A sister group relationship between *Cophosaurus* and *Holbrookia* occurs in two of the alternative hypotheses (Topologies I and II) and is favored by 12 of 15 data partitions or combinations thereof under likelihood (Table 4), including the one (C1 + C2 + C3 + stem + loop) that best explains the data. It is also favored by parsimony analysis of the cyt *b* data and by parsimony analysis of the combined cyt *b* plus 12S data (Fig. 7b). Given the agreement of our results with those of recent analyses based on morphological, allozymic, and DNA hybridization data (Cox and Tanner, 1977, Etheridge and de Queiroz, 1988; de Queiroz, 1989, 1992; Changchien, 1996; Reeder and Wiens, 1996), the sister group relationship between *Cophosaurus* and *Holbrookia* and the single evolution of the concealed tympanic membrane must be considered the best supported of the four alternative hypotheses (Fig. 1).

Lower-Level Relationships

Both cyt *b* and 12S sequences provide support for lower-level relationships among sand lizards—that is, for relationships involving monophyly of the taxa traditionally ranked as genera (or simply named as formal taxa) and particularly for relationships within those taxa.

Uma.—The cyt *b* bootstrap analyses indicate strong support (95%) for a monophyletic *Uma.* For the 12S data, *Uma* is one of two traditional genera for which monophyly is supported by <50% of the bootstrap replicates under both parsimony and likelihood; however, this situation probably reflects the limited ability of the 12S data to resolve deeper divergences within the sand lizard clade. In addition to the strong support provided by the cyt *b* data, monophyly of *Uma* is supported by at least eight unambiguous morphological characters (de Queiroz, 1989). Moreover, genetic distances between the two major clades within *Uma* are all ≥0.075, whereas all strongly supported relationships in the 12S tree (Fig. 6) involve taxa for which genetic distances do not exceed 0.069. Within *Uma*, the cyt *b* and 12S data sets recover nearly the same putative clades with similar bootstrap support. These include a sister group relationship between *U. exsul* and *U. paraphygus* (cyt *b*, 100%; 12S, 99%); monophyly of a group composed of *U. scoparia*, *U. notata*, and *U. inornata* (cyt *b*, 92%; 12S, 77%); and monophyly of a group composed of *U. notata* and *U. inornata* (cyt *b*, 98%; 12S, 66%). The cyt *b* data also support a sister group relationship between *U. notata notata* and *U. inornata* (99%). In agreement with Adest (1977) and de Queiroz (1989, 1992), our analyses support a relatively large separation between the *Uma* of the Mojave and Sonoran deserts (*U. notata*, *U. inornata*, and *U. scoparia*) and those of the Chihuahuan Desert (*U. paraphygas* and *U. exsul*). Within the former (*notata*) group, authors have recognized one (Schmidt, 1953; Adest, 1977), two (e.g., Norris, 1958; Carpenter, 1963), or three (Mayhew, 1964; Pough, 1973, 1974, 1977) species. The cyt *b* distances between *U. scoparia* and *U. notata–inornata* (0.113–0.127) are within the range of other between-species comparisons in this study. In contrast, the cyt *b* distances between *U. notata* and *U. inornata* (0.009–0.020) are low even for within-species comparisons, though the taxa are morphologically distinguishable and are sometimes recognized as separate species (e.g., Mayhew, 1964; Pough, 1973, 1974, 1977). Interestingly, our results indicate that *U. notata* is paraphyletic, with *U. notata notata* being more closely related to *U. inornata* than to *U. notata rufopunctata*, and highlight the need for a detailed investigation of these three forms.

Callisaurus.—We observed strong to support (cyt *b*, 100%; 12S, 97%) for a monophyletic *Callisaurus*, corroborating the results of an earlier allozyme study (de Queiroz, 1992). The cyt *b* data support three major clades within the single currently recognized species *Callisaurus draconoides*, two of which are also supported by the 12S data, whereas the third is not contradicted by them. Specimens from Sonora and Sinaloa, representing the taxa *Callisaurus d. bogerti*, *brevipes*, or *inusitatus* (CDSS) and *C. d. bogerti*, form a strongly (cyt *b*, 95%) to weakly (12S, 64%) supported clade the placement of which as sister to all other *Callisaurus* is weakly supported (cyt *b*, 68%; 12S, <50%) by the

likelihood analyses but is contradicted by the cyt *b* parsimony analysis when transitions are downweighted 2:1: That is, 54% of the bootstrap replicates support the placement of the Baja California taxa (*C. d. crinitis* and *C. d. carmenensis*) as sister taxa to all other *Callisaurus*. In the likelihood analysis, the Baja California clade is strongly supported (95%) by the cyt *b* data but not by the 12S data. A clade of the three northern samples, representing *C. d. myurus*, *C. d. rhodostictus*, and *C. d. ventralis*, is supported strongly by cyt *b* (96%) and weakly by 12S (56%). Within the later clade, the Mojave sample of *C. d. rhodostictus* forms a clade with *C. d. myurus* that has strong (cyt *b*, 90%) to weak (12S, <50%) support. At least some of the cyt *b* genetic distances between the three clades (0.093–0.117) are within the range of between-species comparisons observed among other sand lizards, whereas all 12S distances (0.006–0.037) are within the range of within-species comparisons.

Cophosaurus.—Our data provide strong support for monophyly of the two *Cophosaurus* samples, representing *C. t. texanus* and *C. t. scitulus*. Because we did not sample the third *Cophosaurus* subspecies (*C. t. reticulatus*), this result should not be taken as evidence for monophyly of the species as a whole. The distances between the *C. t. texanus* and *C. t. scitulus* (cyt *b*, 0.055; 12S, 0.041) are similar to those observed within other species in this study.

Holbrookia.—The cyt *b* data provide weak support (63%) for the monophyly of *Holbrookia*. The likelihood analysis of the 12S data did not support *Holbrookia* monophyly in >50% of the bootstrap replicates, though the taxon is monophyletic in all of the 15 ML topologies (Fig. 4c) and all of the six MP topologies (Fig. 4b). Within *Holbrookia*, our analyses strongly support (cyt *b*, 100%; 12S, 98%) a monophyletic *Holbrookia lacerata* and show moderate support (cyt *b*, 84%) to weak (12S, <50%) for its placement as the sister taxon of all other *Holbrookia*, that is, *H. maculata* and *H. propinqua*. In contrast, monophyly of *H. maculata* is contradicted by the cyt *b* data. The northeastern populations of this taxon (*H. m. maculata*, *H. m. campi*, *H. m. flavilenta*, *H. m. ruthveni*, and *H. m. bunkeri*) appear more closely related to *Holbrookia propinqua* than to the southwestern populations (*H. m. elegans* and *H. m. thermophila*), though support is weak (56%). The 12S data are unable to resolve the placement of *H. propinqua* relative to the various populations of *H. maculata*, in that neither likelihood nor parsimony bootstrap analyses find any resolution in more than 50% of the replicates. Moreover, the placement of *H. propinqua* in the likelihood analysis is incongruent with its placement in the parsimony analysis, in that each of the 15 ML trees (Fig. 4c) places *H. propinqua* outside of *H. maculata*, whereas the six MP trees (Fig. 4b) place it as sister group of the southwestern populations (*H. m. elegans* and *H. m. thermophila*). Monophyly of the northeastern populations of *H. maculata* is strongly supported by the cyt *b* data (93%), but only the parsimony analyses of the 12S data show >50% bootstrap support for this putative clade. Within this clade, the cyt *b* data provide moderate to strong support (75–98%) for three nested clades, though the most inclusive one is contradicted by two of the weighted parsimony analyses: Downweighting transitions by 10:3 and 5:1 under parsimony provides weak support (52% and 56%, respectively) for a clade composed of all of the taxa except *H. m. campi*; the ML topology excludes *H. m. maculata* instead (Figure 5). *Holbrookia maculata elegans* and *H. m. thermophila* also form a moderately (cyt *b*, 80%) to strongly (12S, 88%) supported clade. Genetic distances between the southwestern and northeastern clades within the currently recognized species *H. maculata* (cyt *b*, 0.176–0.208; 12S, 0.037–0.052) are comparable with those between each of these clades and *H. propinqua* (cyt *b*, 0.161–0.200; 12S, 0.044–0.069) as well as other between-species comparisons. Those within the southwestern (cyt *b*, 0.125; 12S, 0.019) and northeastern (cyt *b*, 0.014–0.063; 12S, 0.003–0.025) clades are comparable with other within-species comparisons. Of particular importance is the fact that the geographically proximate samples of *H. m. thermophila* and *H. m. flavilenta* from Cochise Co., Arizona, exhibit considerably greater distances from one another (cyt *b*, 0.190; 12S, 0.044) than from geographically more distant samples in the larger clades to which they belong (cyt *b*, 0.025–0.125; 12S, 0.009–0.025). A more detailed study of geographic variation with *Holbrookia* is currently in progress.

Heterogeneous Processes

The molecular sequences presented here provide useful data for reconstructing phylogenetic relationships both among and within the species of phrynosomatid sand lizards. The cyt *b* sequences are useful for reconstructing both shallow and deep divergences within this clade, whereas the 12S sequences are useful for reconstrucing shallow divergences. Although not decisive, these data add further support to one of the four alternative hypotheses (Fig. 1) that have been proposed concerning early cladogenetic events within the phrynosomatid sand lizards (topology I), as well as providing new information on more recent cladogenetic events and patterns of genetic and geographic differentiation within species.

Our results also highlight the heterogeneity of molecular sequence evolution and the concomitant importance of developing phylogenetic methods that allow analysis under heterogeneous models. Optimization of likelihood models for the different gene fragments (cyt *b* and 12S) and the structural and functional regions (stem and loop) or classes of sites (codon positions) within those gene fragments revealed pronounced differences among the parameters used to characterize sequence evolution (e.g., base substitution rates, proportion of invariant sites, and rate heterogeneity among sites). When these differences were ignored (i.e., by not partitioning the data), estimates of model parameters yielded intermediate values that in some cases differed greatly from those estimated for one or more subsets of the data (Table 2). Consequently, attempting to characterize all the available data with a single set of model parameters resulted in a considerably lower value for the overall likelihood score. Bull et al. (1993) cautioned against combining data sets where there is significant variation in the underlying processes of sequence evolution. Our approach takes advantage of an important property of likelihood (i.e., the additivity of likelihood values from seperate subsets of data), thereby permitting us to combine data sets while at the same time allowing for variation in the processes acting on them. In the present study, our use of this approach was restricted to evaluating phylogenetic hypotheses defined a priori because available computer programs did not permit searching for optimal trees by using different models and parameter estimates for different subsets of the data. Since then, the ability to search for optimal trees under heterogeneous models has become available in PAML (Yang, 1999), and similar capabilities are being developed in PAUP* (D. L. Swofford, pers. comm.). Further development of such capabilities should greatly improve estimates of phylogeny based on large, heterogeneous data sets, including sequences from both single and multiple genes.

ACKNOWLEDGMENTS

We thank J. O'Brien, J. Gauthier, R. Montanucci, R. Seib, J. Losos, A. Bauer, D. Brown, G. Adest, D. Morafka, R. Murphy, T. Reeder, D. Good, C. Phillips, D. Cannatella, J. Trochet, M. Morris, and S. Walker for providing or helping to collect specimens. J. Sullivan, C. Sutton, J. Huelsenbeck, and D. Swofford provided valuable assistance with the maximum likelihood analyses, and C. Gordon, T. Reeder, and C. Huddleston contributed to the collection of the sequence data. We thank T. Reeder and J. Wiens for insightful comments on an earlier version of this manuscript. This work was partially supported by the Laboratory of Molecular Systematics of the Smithsonian Institution.

REFERENCES

ADACHI, J., AND M. HASEGAWA. 1992. MOLPHY: Programs for molecular phylogenetics I—PROTML: Maximum likelihood inference of protein phylogeny. Computer Science Monograph 27. Institute of Statistics and Mathematics, Tokyo.

ADEST, G. A. 1977. Genetic relationships in the genus *Uma* (Iguanidae). Copeia 1977:47–52.

ADEST, G. A. 1978. The relationships of the sand lizards *Uma*, *Callisaurus*, and *Holbrookia* (Sauria: Iguanidae): An electrophoretic study. Ph.D. Dissertation, Univ. California, Los Angeles.

ANDERSON, S., A. T. BANKIER, B. G. BARRELL, M. H. L. DE BRUIJN, A. R. COULSON, J. DROUIN, I. C. EPERON, D. P. NIERLICH, B. A. ROE, F. SANGER, P. H. SCHREIER, A. J. H. SMITH, R. STADEN, AND I. G. YOUNG. 1981. Sequence and organization of the human mitochondrial genome. Nature 290:457–465.

AXTELL, R. W. 1958. A monographic revision of the iguanid genus *Holbrookia*. Ph.D. Dissertation, Univ. Texas, Austin.

BLACKBURN, D. G. 1978. The comparative, functional, and evolutionary myology of burrowing sceloporine lizards. M.S. Thesis, Cornell Univ., Ithaca, New York.

BULL, J. J., J. P. HUELSENBECK, C. W. CUNNINGHAM, D. L. SWOFFORD, AND P. J. WADDELL. 1993. Partitioning and combining data in phylogenetic analysis. Syst. Biol. 42:384–397.

CARPENTER, C. C. 1963. Patterns of behavior in three forms of the fringe-toed lizards (*Uma*–Iguanidae). Copeia 1963:406–412.

CHANGCHIEN, L.-L. 1996. A phylogenetic study of sceloporine lizards and their relationships with other iguanid lizards based on DNA/DNA hybridization. Ph.D. Dissertation, Univ. Wisconsin Madison.

CHIPPINDALE, P. T., AND J. J. WIENS. 1994. Weighting, partitioning, and combining characters in phylogenetic analysis. Syst. Biol. 43:278–287.

CLARKE, R. F. 1965. An ethological study of the iguanid lizard genera *Callisaurus, Cophosaurus*, and *Holbrookia*. Emporia State Res. Stud. 13:1–66.

COLLINS, T. M., P. H. WIMBERGER, AND G. J. P. NAYLOR. 1995. Compositional bias, character-state bias, and character-state reconstruction using parsimony. Syst. Biol. 43:482–492.

COX, D. R., AND D. V. HINKLEY. 1974. Theoretical statistics. Chapman and Hall, London.

COX, D. C., AND W. W. TANNER. 1977. Osteology and myology of the head and neck regions of *Callisaurus, Cophosaurus, Holbrookia*, and *Uma* (Reptilia: Iguanidae). Great Basin Nat. 37:35–56.

CUNNINGHAM, C. W., H. ZHU, AND D. M. HILLIS. 1998. Best-fit maximum-likelihood models for phylogenetic inference: Empirical tests with known phylogenies. Evolution 52:978–987.

DE QUEIROZ, K. 1989. Morphological and biochemical evolution in the sand lizards. Ph.D. Dissertation, Univ. California, Berkeley.

DE QUEIROZ, K. 1992. Phylogenetic relationship and rates of allozyme evolution among the lineages of sceloporine sand lizards. Biol. J. Linn. Soc. 45:333–362.

DE QUEIROZ, A., M. J. DONOGHUE, AND J. KIM. 1995. Separate versus combined analysis of phylogenetic evidence. Annu. Rev. Ecol. Syst. 26:657–681.

DIXON, M. T., AND D. M. HILLIS. 1993. Ribosomal RNA secondary structure: Compensatory mutations and implications for phylogenetic analysis. Mol. Biol. Evol. 10:256–267.

EARLE, A. M. 1961. The middle ear of *Holbrookia* and *Callisaurus*. Copeia 1961:405–410.

EARLE, A. M. 1962. The middle ear of the genus *Uma* compared to those of the other sand lizards. Copeia 1962:185–188.

EDWARDS, A. W. F. 1972. Likelihood. Cambridge Univ. Press, Cambridge, England.

ETHERIDGE, R., AND K. DE QUEIROZ. 1988. A phylogeny of Iguanidae. Pages 283–367 *in* Phylogenetic relationships of the lizard families (R. Estes and G. Pregill, eds.). Stanford Univ. Press, Stanford, California.

FELSENSTEIN, J. 1978. Cases in which parsimony and compatibility methods will be positively misleading. Syst. Zool. 27:401–410.

FELSENSTEIN, J. 1985. Confidence limits on phylogeny: An approach using the bootstrap. Evolution 39:783–789.

FRATI, F., C. SIMON, J. SULLIVAN, AND D. L. SWOFFORD. 1997. Evolution of the mitochondrial cytochrome oxidase II gene in *Collembola*. J. Mol. Evol. 44:145–158.

GAUT, B. S., AND P. O. LEWIS. 1995. Success of maximum likelihood phylogeny inference in the four-taxon case. Mol. Biol. Evol. 12:152–162.

GU, X., Y.-X. FU, AND W.-H. LI. 1995. Maximum likelihood estimation of the heterogeneity of substitution rate among nucleotide sites. Mol. Biol. Evol. 12:546–557.

HASEGAWA, M., H. KISHINO, AND T. YANO. 1985. Dating the human–ape split by a molecular clock of mitochondrial DNA. J. Mol. Evol. 22:160–174.

HICKSON, R. E., C. SIMON, A. COOPER, G. S. SPICER, J. SULLIVAN, AND D. PENNY. 1996. Conserved sequence motifs, alignment, and secondary structure for third domain of animal 12S rRNA. Mol. Biol. Evol. 13:150–169.

HILLIS, D. M., A. LARSON, S. K. DAVIS, AND E. A. ZIMMER. 1990. Nulceic acids III: Sequencing. Pages 318–370 *in* Molecular systematics, 1st edition (D. M. Hillis and C. Moritz, eds.). Sinauer, Sunderland, Massachusetts.

HILLIS, D. M., B. K. MABLE, AND C. MORITZ. 1996. Applications of molecular systematics: The state of the field and a look to the future. Pages 515–543 *in* Molecular systematics, 2nd edition (D. M. Hillis, C. Moritz, and B. K. Mable, eds.). Sinauer, Sunderland, Massachusetts.

HUELSENBECK, J. P. 1995. Performance of phylogenetic methods in simulation. Syst. Biol. 44:17–48.

HUELSENBECK, J. P., AND J. J. BULL. 1996. A likelihood ratio test to detect conflicting phylogenetic signal. Syst. Biol. 45:92–98.

HUELSENBECK, J. P., D. L. SWOFFORD, C. W. CUNNINGHAM, J. J. BULL, AND P. J. WADDELL. 1994. Is character weighting a panacea for the problem of data heterogeneity in phylogenetic analysis? Syst. Biol. 43:288–291.

IRWIN, D. M., T. D. KOCHER, AND A. C. WILSON. 1991. Evolution of the cytochrome *b* gene of mammals. J. Mol. Evol. 32:128–144.

JAMES, B. D., G. J. OLSEN, J. LIU, AND N. R. PACE. 1988. The secondary structure of ribonuclease P RNA, the catalytic element of a ribonucleoprotein enzyme. Cell 52:19–26.

JONES, T. R., W. R. TAYLOR, AND J. M. THORNTON. 1992. The rapid generation of mutation data matrices from protein sequences. Comput. Appl. Biosci. 8:25–282.

JUKES, T. H., AND C. R. CANTOR. 1969. Evolution of protein molecules. Pages 21–132 *in* Mammalian protein metabolism (H. N. Munro, ed.). Academic Press, New York.

KIMURA, M. 1980. A simple method for estimating evolutionary rate of base substitution through comparative studies of nucleotide sequences. J. Mol. Evol. 16:111–120.

KISHINO, H., AND M. HASEGAWA. 1989. Evaluation of the maximum likelihood estimate of the evolutionary tree topologies from DNA sequence data, and the branching order in Hominoidea. J. Mol. Evol. 29:170–179.

KJER, K. M. 1995. Use of rRNA secondary structure in phylogenetic studies to identify homologous positions: An example of alignment and data presentation from the frogs. Mol. Phylogenet. Evol. 4:314–330.

KORNEGAY, J. R., T. D. KOCHER, L. A. WILLIAMS, AND A. C. WILSON. 1993. Pathways of lysozyme evolution inferred from the sequences of cytochrome *b* in birds. J. Mol. Evol. 37:367–379.

KRAUS, F., L. JARECKI, M. M. MIYAMOTO, S. M. TANHAUSER, AND P. J. LAIPIS. 1992. Mispairing and compensational changes during the evolution of mitochondrial ribosomal RNA. Mol. Biol. Evol. 9:770–774.

KUMAZAWA, Y., H. OTA, M. NISHIDA, AND T. OZAWA. 1998. The complete nucleotide sequence of a snake (*Dinodon semicarinatus*) mitochondrial genome with two identical control regions. Genetics 150:313–329.

MARTIN, A. P., AND S. R. PALUMBI. 1993. Protein evolution in different cellular environments: Cytochrome *b* in sharks and mammals. Mol. Biol. Evol. 10:873–891.

MAYHEW, W. W. 1964. Taxonomic status of California populations of the lizard genus *Uma*. Herpetologica 20:170–183.

MITTLEMAN, M. B. 1942. A summary of the iguanid genus *Urosaurus*. Bull. Mus. Comp. Zool. Harvard Univ. 91:106–176.

NAYLOR, G. J. P., AND W. M. BROWN. 1998. *Amphioxus* mitochondrial DNA, chordate phylogeny, and the limits of inference based on comparisons of sequences. Syst. Biol. 47:61–76.

NIELSEN, R. 1997. Site-by-site estimation of the rate of substitution and the correlation of rates in mitochondrial DNA. Syst. Biol. 46:346–353.

NORRIS, K. S. 1958. The evolution and systematics of the iguanid genus *Uma* and its relation to the evolution of other North American desert reptiles. Bull. Am. Mus. Nat. Hist. 114:253–326.

NUNN, G. B., J. COOPER, P. JOUVENTIN, C. J. R. ROBERTSON, AND G. G. ROBERTSON. 1996. Evolutionary relationships among extant albatrosses (Procellariiformes: Diomedeidae) established from complete cytochrome-*b* gene sequences. Auk 113:784–801.

NUNN, G. B., AND J. CRACRAFT. 1996. Phylogenetic relationships among the major lineages of the birds-of-paradise (Paradisaeidae) using mitochondrial DNA gene sequences. Mol. Phylogenet. Evol. 5:445–459.

PORTER, C. A., M. W. HAIDUK, AND K. DE QUEIROZ. 1994. Evolution and phylogenetic significance of ribosomal gene location in chromosomes of squamate reptiles. Copeia 1994:302–313.

POUGH, F. H. 1973. *Uma inornata*. Cat. Am. Amphib. Reptiles 126:1–2.

POUGH, F. H. 1974. *Uma scoparia*. Cat. Am. Amphib. Reptiles 155:1–2.

POUGH, F. H. 1977. *Uma notata*. Cat. Am. Amphib. Reptiles 197:1–2.

RASSMANN, K. 1997. Evolutionary age of the Galapagos iguanas predates the age of the present Galapagos Islands. Mol. Phylogenet. Evol. 7:158–172.

REEDER, T. W. 1995. Phylogenetic relationships among phrynosomatid lizards as inferred from mitochondrial ribosomal DNA sequences: Substitutional bias and information content of transitions relative to transversions. Mol. Phylogenet. Evol. 4:203–222.

REEDER, T. W., AND J. J. WIENS. 1996. Evolution of the lizard family Phrynosomatidae as inferred from diverse types of data. Herpetol. Monogr. 10:43–84.

RICHARDS, C. M., AND W. S. MOORE. 1996. A phylogeny for the African treefrog family Hyperoliidae based on mitochondrial rDNA. Mol. Phylogenet. Evol. 5:522–532.

ROUSSET, F., M. PELANDAKIS, AND M. SOLIGNOC. 1991. Evolution of compensatory substitutions through G-U intermediate state in *Drosophila* rRNA. Proc. Natl. Acad. Sci. USA 88:10032–10036.

SAS INSTITUTE. 1990. SAS, version 6. SAS Institute, Cary, North Carolina.

SAVAGE, J. M. 1958. The iguanid lizard genera *Urosaurus* and *Uta*, with remarks on related groups. Zoologica 43:41–54.

SCHMIDT, K. P. 1953. A checklist of North American amphibians and reptiles, 6th edition. American Society of Ichthyologists and Herpetologists, Chicago, Illinois.

SIMON, C., L. NIGRO, J. SULLIVAN, K. HOLSINGER, A. MARTIN, A. GRAPPUTO, A. FRANKE, AND C. MCINTOSH. 1996. Large differences in substitutional pattern and evolutionary rates of 12S ribosomal RNA genes. Mol. Biol. Evol. 13:923–932.

SMITH, H. M. 1946. Handbook of lizards. Comstock, Ithaca, New York.

SULLIVAN, J. 1996. Combining data with different distributions of among-site rate variation. Syst. Biol. 45:375–380.

SULLIVAN, J., AND D. L. SWOFFORD. 1997. Are guinea pigs rodents? The importance of adequate models in molecular phylogenetics. J. Mammal. Evol. 4: 77–86.

SULLIVAN, J., K. E. HOLSINGER, AND C. SIMON. 1995. Among-site rate variation and phylogenetic analysis of 12S rRNA in sigmodontine rodents. Mol. Biol. Evol. 12:988–1001.

SULLIVAN, J., K. E. HOLSINGER, AND C. SIMON. 1996. The effect of topology on estimates of among-site rate variation. J. Mol. Evol. 42:308–312.

SWOFFORD, D. L., G. J. OLSEN, P. J. WADDELL, AND D. M. HILLIS. 1996. Phylogenetic inference. Pages 407–514 *in* Molecular systematics, 2nd edition (D. M. Hillis, C. Moritz, and B. K. Mable, eds.). Sinauer, Sunderland, Massachusetts.

THOMPSON, J. D., D. G. HIGGINS, AND T. J. GIBSON. 1994. Clustal W: Improving the sensitivity of progressive multiple sequence alignment through sequence weighting, position-specific gap penalties and weight matrix choice. Nucleic Acids Res. 22:4673–4680.

WADDELL, P. J., AND D. PENNY. 1996. Evolutionary trees of apes and humans from DNA sequences. Pages 53–73 *in* Handbook of symbolic evolution (A. J. Lock and C. R. Peters, eds.). Clarendon Press, Oxford, England.

WAKELEY, J. 1996. The excess of transitions among nucleotide substitutions: New methods of estimating transition bias underscore its significance. Trends Ecol. Evol. 11:158–163.

WOLFE, A. C., P. M. SHARP, AND W.-H. LI. 1989. Mutation rates differ among regions of the mammalian genome. NATURE 337:283–285.

YANG, Z. 1994a. Estimating the pattern of nucleotide substitution. J. Mol. Evol. 39:105–111.

YANG, Z. 1994b. Maximum likelihood phylogenetic estimation from DNA sequences with variable rates over sites: Approximate methods. J. Mol. Evol. 39:306–314.

YANG, Z. 1996a. Among-site rate variation and its impact on phylogenetic analyses. Trends Ecol. Evol. 11:367–372.

YANG, Z. 1996b. Phylogenetic analysis using parsimony and likelihood methods. J. Mol. Evol. 42:294–307.

YANG, Z. 1999. Phylogenetic Analysis by Maximum Likelihood (PAML), Version 2.0. University College London.

YANG, Z., N. GOLDMAN, AND A. FRIDAY. 1995a. Maximum likelihood trees from DNA sequences: A peculiar statistical estimation problem. Syst. Biol. 44:384–399.

YANG, Z., I. J. LAUDER, AND H. J. LIN. 1995b. Molecular evolution of the hepatitus B virus genome. J. Mol. Evol. 41:587–596.

Received 12 January 1999; accepted 8 April 1999
Associate Editor: J. Wiens